# Nonbound dislocations in hexagonal patterns: pentagon lines in surface-tension-driven Bénard convection

Kerstin Eckert[1] and André Thess[2]
[1]*Institute for Aerospace Engineering, Dresden University of Technology, 01062 Dresden, Germany*
[2]*Department of Mechanical Engineering, Ilmenau University of Technology, P.O. Box 100565, 98684 Ilmenau, Germany*
(Received 5 December 1997; revised manuscript received 10 June 1999)

We report on a novel class of defects in a hexagonal pattern which we call pentalines. They are built up of two nonbound dislocations and are orientated parallel to the roll axis of the mode free of a dislocation. A pentaline has its origin in a transformation of the penta-hepta defect (PHD), taking place at higher supercriticality. The underlying mechanism consists in a combination of glide and climb motion of the original dislocations bound to the PHD. We demonstrate that the pentalines play an important role within the transition from hexagonal towards square convection cells, observed in surface-tension-driven Bénard convection. [S1063-651X(99)06310-2]

PACS number(s): 47.54.+r, 47.20.Dr

## I. INTRODUCTION

Defects strongly influence the dynamics of hydrodynamic systems. Impressive examples are the change of the characteristic macroscopic length scale due to the defect motion (e.g., [1,2]) and the mediating of the transition to a weakly turbulent state [3,4], or to a pattern with different symmetry [5–9]. The defect type which has been studied most extensively is the dislocation in a roll pattern (for an overview see, e.g., [10]). The dislocation represents the generic point defect of the roll pattern and can in principle either move parallel (climb) or perpendicular (glide) to the roll axis. The present paper is concerned with formation and evolution of defects in a hexagonal pattern. Hexagonal patterns are the result of a superposition of three roll systems whereby the angle between them amounts to 120°. We find that changes in the defect structure in such a composite pattern can be traced back to the two elementary types of dislocation motion in the particular modes. Therefore it makes sense to summarize what the results of previous experimental and theoretical studies on pure roll patterns are with respect to the dislocation motion. We first consider the Rayleigh-Bénard convection (RBC). The majority of studies is focused to the climb motion of dislocations. In an early experiment [1] it was shown by means of a row of dislocations that climbing provides a size-adjustment mechanism. The climb velocity was found to be inversely proportional to the Prandtl number of the fluid. (The Prandtl number $\mathrm{Pr}=\nu/\kappa$ is the ratio between the kinematic viscosity $\nu$ and the thermal diffusivity $\kappa$.) This experiment motivated later theoretical studies [11,12]. Both works demonstrate that the climb velocity is proportional to $\delta k^{3/2}$ provided the dynamics can be derived from a potential. Here, $\delta k = k_{opt} - k$ where $k_{opt}$ stands for the wave number at which the dislocation is stationary. For nonpotential systems the climb velocity obeys a linear dependency on $\delta k$ [12]. The uniform climb velocity, predicted by [11], was experimentally verified in [2]. Furthermore, it was shown in [2] that the climb velocity behaves approximately proportional to $\delta k^{3/2}$. At a given $\delta k$, the climb velocity increases with the control parameter.

In contrast to the climb motion, the glide motion occurs only in nonpotential systems [12] and involves nonsymmetric pinching off and reforming of rolls. From the theoretical side, it is therefore much harder to treat than climbing [12]. Presently, an elaborated theory does not exist. Some qualitative features of gliding are given in [13]. Gliding occurs with small and nonuniform velocity and is stopped at high Rayleigh numbers. It is favored if $k \approx k_{opt}$, or if the layer rotates [14]. In the latter work was found that the gliding motion and the subsequent annihilation of defects causes a reorientation of the whole structure.

We briefly turn to anisotropic flows, for which electrohydrodynamic convection (EHC) is an important example. The preparation of well separated defects can be achieved more simply than in RBC which supported a better understanding of the dynamics and interaction of defects in EHC. For an overview we refer to [15]. According to theory [16–18], a dislocation can display both climbing and gliding. Climbing occurs if the wavenumber deviates from the optimal one while gliding is preferred if the rolls are tilted against the normal direction. The motion of a pair of dislocations with opposite charge has been investigated experimentally in [18–21]. The study at vanishing external stresses [21], i.e., at zero wave number mismatch, revealed a universal length scale for both climb and glide motion below which the mutual interaction of defects becomes important. Studies with imposed external stresses show that climbing occurs in two stages [18,20]. At large distances between both defects the velocity is constant. Below a crossover distance the motion accelerates. In contrast to the smooth climbing motion the gliding shows a steplike behavior [18,20]. In accordance with [14] for RBC, the annihilation of dislocations by gliding leads to a reduction of the original tilt angle [19]. This observation supported the idea that the glide motion is a selection process for the pattern orientation.

We now leave the pure roll pattern to turn to defects in the composite hexagonal pattern which recently have attracted attention [22–29]. Typically, hexagonal patterns occur in presence of a vertical asymmetry, caused, e.g., by temperature-dependent material parameters or by a difference between top and bottom boundary conditions. Promi-

 

nent candidates are non-Boussinesq Rayleigh-Bénard convection or surface-tension-driven Bénard convection (STDBC). A number of defects in a hexagonal pattern, as they occur in weakly supercritical STDBC, has been described in [22–24]. Most of them are unstable. They either disappear rapidly, or they transform into the basic penta-hepta defects (PHD). Therefore, the interest of previous works is exclusively focused to this type of defect. In [25] it was shown that a PHD is a bound state of two dislocations of opposite phase circulation in two different roll systems. A theoretical explanation for the existence of this cell compound has been given by a numerical simulation [27] which demonstrated that locally separated dislocations attract each other to form a bound state which is the PHD. The far-field solution for the phase field of a static PHD was found in [26]. This solution has been generalized for a moving PHD in [28,29]. From the analysis of the mobility tensor in these papers followed that the direction of motion of the PHD depends strongly on the deviation of the wave number of the particular modes from their optimal value. So, the PHD is stationary if the wave number of the three modes equals the onset value. It is now widely accepted that the motion of the PHD is an important wave number selection mechanism in a hexagonal pattern.

The evolution of induced perfect hexagonal patterns at moderate supercriticality was investigated in a fluid with Prandtl number $\mathrm{Pr}\sim O(10^3)$ [23]. To achieve its optimal wave number, the pattern chooses different ways depending on the wave number mismatch. For $\delta k<0$ the nucleation of new cells is observed while for $\delta k>0$ the fusion of cells dominates. Both ways introduce defects which dynamics finally lead to the establishment of the optimal wave number. For small $\delta k>0$ and a small container the authors report about the appearance of a dislocation which climbs through the container thereby accelerating the adjustment of the optimal wave number. Unfortunately, no systematic analysis of this effect was given.

While the structure of defects, especially that of the PHD, and their influence on the pattern evolution in the weakly supercritical range is well understood, nothing is known what happens with these defects if the control parameter is increased. Theoretical models, based on amplitude equations, are not capable to cover this range, and we are not aware of experiments tackling this problem for moderate Prandtl numbers $\mathrm{Pr}\sim O(10^2)$. (This Pr-number range has been proven as suitable [7] since the vertical vorticity present at finite Pr is still high enough to ensure a rich defect dynamics.) We remark that the knowledge about the modification in the defect structure is particularly useful with view on the hexagon-square-transition, recently observed in STDBC [5–7,9]. In these works were found that the hexagons become unstable against square convection cells whereby the transition is mediated by pentagonal cells. In the present paper we study the formation of these pentagons. We show that a universal schema exists guiding the transformation of the PHD into an association of pentagonal cells which we call pentaline. Similar to the PHD, the pentaline is built up of two dislocations with opposite winding number. But, in contrast to the PHD, the dislocations are not longer bound together. With advanced stage of the pentaline, the distance of separation between the dislocations increases monotonously. Such a state is forbidden in the weakly supercritical range [27].

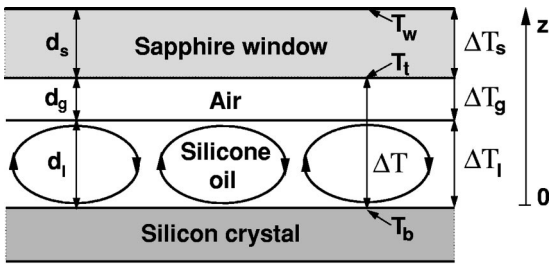


FIG. 1. Schematic of the liquid-air Bénard system: A temperature difference $\Delta T$ is maintained across a two-layer system by isothermal plates. The flow is mainly driven by the temperature dependence of surface tension. $\Delta T_l$ and $\Delta T_g$ represent the average temperature drops in the oil and in the air, respectively. $d_l$ and $d_g$ are the thicknesses of the respective layers. For the definition of the control parameter $\varepsilon$ it is useful to refer to the temperature drop $\Delta T_{cd}$ assuming that both layers are in conductive state (cf. detailed discussion in [7]).

In the following we briefly describe the experiment and the method of analysis. Then we study the decay of the basic PHD into the nucleus of a pentaline and analyze the growth of the pentaline until it reaches its developed stage. The connection between the pentalines and the square convection cells is outlined.

## II. EXPERIMENTAL METHODS

The system under consideration is sketched in Fig. 1. A layer of silicone oil (kinematic viscosity $\nu=0.1\ \mathrm{cm}^2/\mathrm{s}, \mathrm{Pr}=100$) is heated from below. The free surface of the oil is in contact with an air layer, cooled by an upper isothermal plate. The bottom plate of the layer consists of a polished silicon wafer embedded into a massive copper block. The transparent top plate is made of sapphire. In the paper we present the synopsis of numerous experiments, whereby the figures were selected among different experiments to achieve the most clear presentation of the phenomena. The depth $d_l$ of the liquid layer varies in these experiments between 1.08 mm and 1.45 mm which leads to an aspect ratio of $\Gamma=2r/d_l$ between 64 and 80. $r$ stands for the radius of the experimental container. More details about the experiments can be found in Refs. [5,7]. The control parameter $\varepsilon$ of our system is defined as

$$\varepsilon=\frac{\Delta T_{cd}-\Delta T_c}{\Delta T_c} \tag{1}$$

with the *c*on*d*uctive temperature drop

$$\Delta T_{cd}=\frac{Bi}{1+Bi}(T_b-T_t). \tag{2}$$

$\Delta T_c$ is the temperature difference required for onset of convection in hexagonal cells. The Biot number $\mathrm{Bi}=\lambda_g d_l/\lambda_l d_g$ lays between 0.5 and 1, depending on $d_l$ and the depth of the air layer $d_g$ ($0.26\ \mathrm{mm}<d_g<0.40\ \mathrm{mm}$). $\lambda_g$ and $\lambda_l$ are the heat conductivities of air and liquid, respectively. The hexagonal convective pattern is analyzed by means of the shadowgraph-technique. The shadowgraph in-

tensity G(x,y) may be written as sum over the intensities delivered by the three modes, i.e.,

$$G(x,y)=\sum_{j=1}^{3} A_j(x,y)\exp(\mathrm{i}\mathbf{k_j}\cdot\mathbf{r})+c.c. \tag{3}$$

The information about the defect structure is entirely contained in the amplitudes $A_j$ which are slowly varying functions across the pattern. To obtain the $A_j$ we apply the Fourier-demodulation-technique [20,25]. After having determined the $\mathbf{k_j}$ (j=1,2,3) we shift the Fourier-spectrum by $-\mathbf{k_j}$. The particular peak is now located in the origin of the co-ordinate system. The remaining part of the spectrum is filtered out by using the following isotropic low-pass-filter [30]

$$\mathbf{B}^{(n,l)}=\mathbf{B}_1^{(n,l)}\mathbf{B}_2^{(n,l)}\mathbf{B}_3^{(n,l/4)}\mathbf{B}_4^{(n,l/4)} \tag{4a}$$

with

$$\mathbf{B}_{1,2}^{(n,l)}=\left(1-\frac{1}{2^n}[1-\cos(\pi\tilde{k}_i)]^n\right)^l \tag{4b}$$

and $i=(x,y)$,

$$\mathbf{B}_{3,4}^{(n,l/4)}=\left(1-\frac{1}{2^n}\left[1-\cos\frac{\pi}{\sqrt{2}}(\tilde{k}_x\pm\tilde{k}_y)\right]^n\right)^{l/4}, \tag{4c}$$

where $\tilde{k}_i$ is the wave number $k_i$ normalized by the Nyquist frequency. The filter degree $n$ determines the slope of the filter. The exponent $l$ fixes the cutoff wavenumber. Inverse Fourier transformation yields then the complex amplitude $A_j$. The position of the core of a dislocation follows from the condition $\mathrm{Re}A_j=\mathrm{Im}A_j=0$. The points where the lines of vanishing real $\mathrm{Re}A_j$ and imaginary parts $\mathrm{Im}A_j$ intersect each other are detected numerically. To obtain the roll structure of mode $j$ the filtered spectrum is shifted back by $+\mathbf{k}_\mathrm{j}$ and inverse Fourier transformed. This procedure is repeated for all three modes. Minima and maxima of the roll systems are again determined numerically. In the following chapters, the lines of minimal intensity are superimposed to the pattern to display the composition of the studied defects.

A comment is in order regarding the influence of varying filter sizes onto the results. In the $k_j$ and $\varepsilon$ ranges where experiments run, the distance between adjacent peaks is rather small. Additionally, a splitting of one peak into two subpeaks can occur due to the presence of defects. These conditions require a careful choice of the filter size. A to small filter degree $n$ in combination with a large value of $l$ can destroy information of the mode under study. To high $n$ or to small $l$ are not efficient in filtering out the other modes. Typically, we choose $n=2$ and $l=2^m$ where $m$ depends on the size of the cells, i.e., on $d_l$. Since the choice of $n$ and $l$ is not unique we have systematically checked their effect on the location of the dislocation cores. For reasonable $(n,l)$ combinations we found an uncertainty of less than one-half of a hexagon side length. So, the results are effectively invariant against minor changes of the filter size.

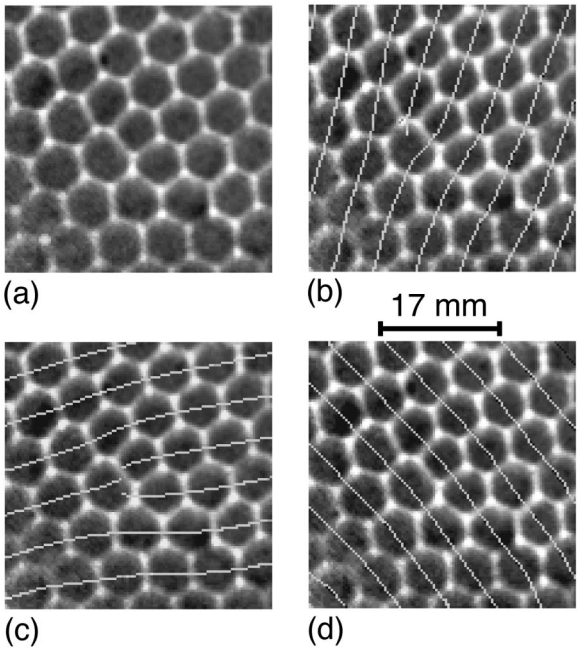


FIG. 2. The penta-hepta defect (a) and its decomposition into the three roll subsystems. Roll set 1 (b) and 2 (c) contain a dislocation which differs in the phase circulation. The white lines superimposed on the shadowgraph image in (b)–(d) represent the lines of minimal intensity of the particular roll pattern obtained by Fourier demodulation.

## III. THE TRANSFORMATION OF THE PENTA-HEPTA DEFECT

First, we briefly consider the basic features of a penta-hepta defect because of the important role which this defect plays in the scenario to be described. The PHD is a bound state of two dislocations of opposite circulation of the phase, $\phi(x,y)$, i.e., $1/(2\pi)\oint_C\nabla\phi(x,y)d\mathbf{s}=\pm\mathbf{1}$, in two different roll systems [25]. $C$ is a closed contour encircling the core of the dislocation. In our notation, a dislocation has a charge of $+1$ when the phase jump is $+2\pi$, gone in counterclockwise direction. In Fig. 2 we show a PHD with dislocations in the modes 1 and 2 and no dislocation in mode 3. The two dislocation cores are localized within the heptagon, close to the joint cell edge with the pentagon in accordance with [25]. Exactly, six different PHD can occur; obtained by permutation of the charges of the dislocations. Without loss of generality we concentrate in the following to a PHD of $(-1,1,0)$ type.

Let us study what happens with a PHD if we increase the control parameter $\varepsilon$. We observe the PHD up to $\varepsilon\sim4$ in our experiments. Its stability, however, is reduced in comparison with the range of small $\varepsilon$. To illustrate this we look into the behavior of the (normalized) numbers $p_i=N_i/N$ of hexagons $(i=6)$ and pentagons $(i=5)$ shown in Fig. 3. $N_i$ and $N$ denote the number of cells of a particular cell class and the total number of cells, respectively. We find a growing number of pentagons above $\varepsilon\sim2$. That means a mechanism must exist transferring cells of hexagonal into pentagonal planform. We wish to demonstrate that the PHD plays a key role within this process. The mobility of the PHD is limited in this $\varepsilon$ range which can be attributed to pinning effects by the underlying small-scale structure [12,14,18,31]. So the PHD

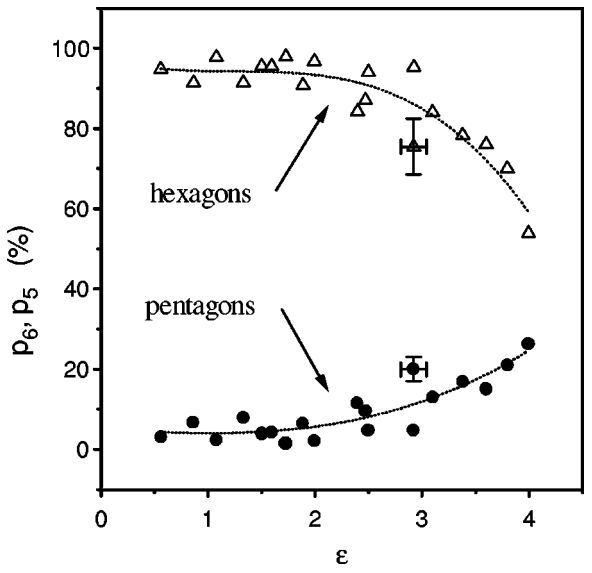


FIG. 3. The number (normalized) of pentagonal cells $p_5$ and of hexagonal cells $p_6$ as function of the control parameter $\varepsilon$. Note that $p_5$ begins to grow continuously at $\varepsilon > 2(\mathrm{Pr}=100)$.

can no longer contribute to the wave number selection by its motion. But the PHD could support local changes of the wave number by a modification of its shape. That is exactly what the PHD does: it decays in a continuous process which is sketched in Fig. 4. Above $\varepsilon \sim 2$, the heptagon of the PHD shows a tendency to diminish one cell side close to the pentagon [Fig. 4(b)] until two of the seven cell knots merge [Fig. 4(c)]. As a result, a cell compound, the 5-5-6-6 cluster, consisting of two pentagons and two nonequilateral hexagons, is formed. This cluster is shown in Fig. 5(a) together with its decomposition in Figs. 5(b)–5(d). The elementary mechanism leading to the formation of a 5-5-6-6 cluster consists in a climb motion of one of the two dislocations, forming the original PHD. Frequently, a glide motion by $\pi/k_i$ precedes that climb motion. This is the case in the concrete example where the dislocation in roll set 2 [Figs. 2(c) and 5(c)] shows a climbing by a distance of approximately one hexagon side length after the gliding. In result, the cell edge of the heptagon perpendicular to this roll line disappears, transforming the heptagon into a hexagon. The dislocation core of this roll set is now localized close to the central vertex of the newly formed 5-5-6-6 cluster. [This vertex has a coordination number 4 (four edges incident), as opposed to the other cell knots which are vertices of coordination number 3.] By contrast, the core of the dislocation in roll set 1 [Figs. 2(b) and 5(b)] stays nearly unchanged close to the shortest side of the left nonequilateral hexagon 5-5-6-6 cluster. Roll set 3 remains again free of a dislocation. The distance of separation between both dislocation cores amounts to approximately two average hexagon side lengths. The existence of two *nonbound* dislocations is the basic difference between the 5-5-6-6 cluster and the PHD. Such a state is impossible in the weakly supercritical range because the dislocations become attracted towards each other [27]. But in the moderately supercritical range, the 5-5-6-6 cluster is the dominant defect type which can clearly be recognized already in the old original photographs of Bénards experiment (Fig. 6). Thus, the formation of the 5-5-6-6 clusters and their subsequent evolution can clearly be identified as the reasons for the rise of the pentagon number in Fig. 3.

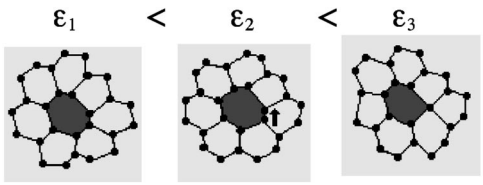


FIG. 4. Beyond $\varepsilon \sim 2$ the heptagon of the PHD (a) shows a tendency to diminish the length of one side adjacent to the pentagon. A deformed PHD appears (b). The shortening of this side continues and the 5-5-6-6 cluster is formed (c). We show details of shadowgraph images converted into binary picture whereby the heptagon is shown in gray.

The scenario of the transformation of the PHD described above represents the generic one. Frequently, however, one will encounter the beginning of pentagon formation in a seemingly different manner. A typical example is given in Fig. 7(a). By means of this example, we wish to show that these alternative ways can be deduced from the generic transformation. With increasing $\varepsilon$ the probability to find isolated PHD's decreases. Moreover, two PHD's are often located side by side, separated by a pentagonal cell, belonging to one of the both PHD's. In the rule, only one PHD starts to tansform into the 5-5-6-6 cluster, the other one will follow at higher $\varepsilon$.This situation is depicted in Fig. 7. From both heptagons of the PHD's (the pentagons belonging to are marked by $P$), the lower one transforms into a hexagon (hatched). The newly formed pentagon is located in between the both

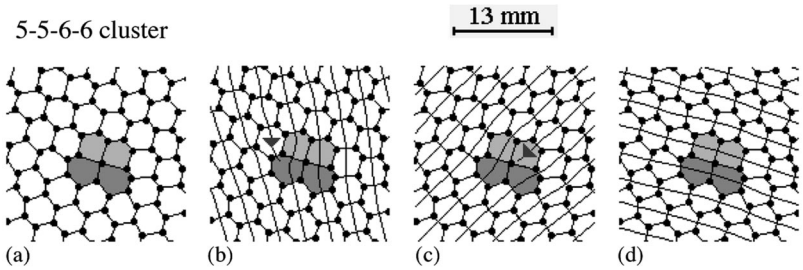


FIG. 5. The 5-5-6-6 cluster (a). This defect is built up of two pentagons (light gray) and two nonequilateral hexagons (dark gray). The 5-5-6-6 cluster is the result of the transformation of the PHD involving a combination of glide and climb motion of the dislocations. The decomposition of this new defect into the roll patterns of the modes $j(j=1,2,3)$ is shown in (b)–(d). Note, that the dislocations in the modes 1 and 2 are separated by a distance of about two average hexagon side lengths. For better visibility, the original shadowgraph image is again converted into a binary picture. Black lines correspond to minimal intensity of the particular roll pattern. Dislocated rolls are marked by arrows.

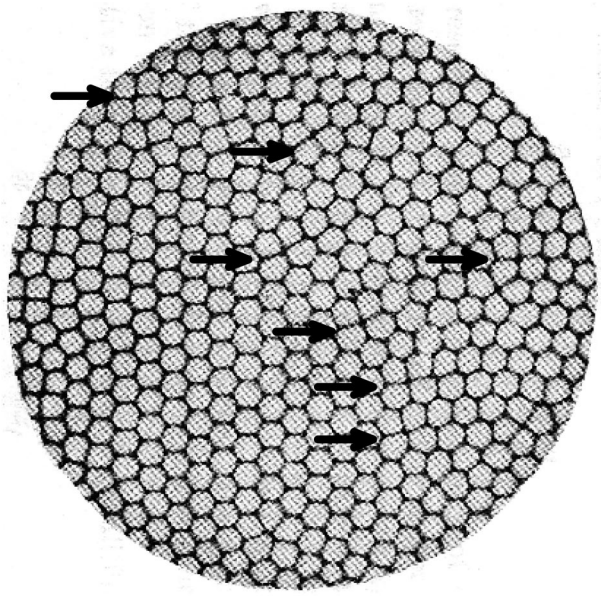

FIG. 6. A reproduction of one of Bénards original photographs [32] displaying numerous 5-5-6-6 cluster marked by arrows.

already existing pentagons. The only difference from the usual 5-5-6-6 clusters consists in the absence of a second nonequilateral hexagon since this place is entered yet by the pentagon of the upper PHD. An interesting feature of this way of pentagon formation consists in the fact that it requires an annihilation of two of the four dislocation, building up the both PHD's. This annihilation takes place via gliding. The surviving two dislocations in the modes $j=1$ and $j=3$ additionally display a climb motion over a distance of about one hexagon side length.

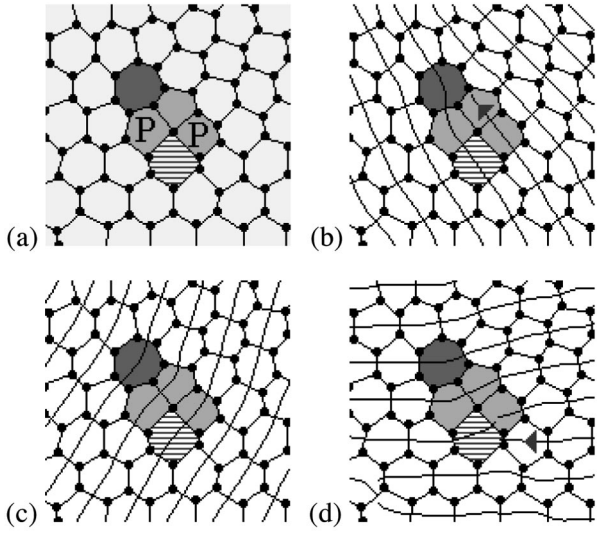


FIG. 7. The formation of pentagons between two PHD's which are separated by one pentagonal cell. Only one of the heptagonal cells (the lower one) undergoes a transformation into a hexagonal cell (hatched) producing a third pentagon. The heptagon not transformed and the pentagons are shown in dark and light gray, respectively. Pentagons belonging to the original PHD's are marked by *P*. From the four dislocations building up the former two PHD's only two of them survive. The other two are annihilated mainly by gliding.

## IV. THE FORMATION OF PENTALINES

Next we address the question of what happens finally with a 5-5-6-6 cluster when $\varepsilon$ is increased. We observe that this defect expands in the same manner as it was created. The expansion proceeds in analogy to the closing of a zipfastener. The shortest side of one of the two hexagons of the cluster begins to shrink until both cell knots merge again. Consequently, two new pentagons are formed. The first one below the two pentagons of the cluster and the other one aside. In parallel, the hexagon adjacent to both new pentagons becomes non-equilateral again. These ensemble is shown in Fig. 8(a). We denote this state as a (1,3)-pentaline since one pentagon is placed below three upper ones. The decomposition of a (1,3)-pentaline into the three roll systems is given in Fig. 8(b-d). The formation of two new pentagons is equivalent to a combined glide/climb motion of one dislocation, comprising the gliding by $2\pi/k_i$ together with a climbing by one to two hexagon side lengths. This mechanism is shown in Fig. 9. This figure makes clear that a discontinuity in the roll line, e.g. observed in Fig. 8(f) is not an artifact but expression of the gliding process. The location of the other dislocation belonging to this cell ensemble remains unchanged. On looking in detail to the rolls surrounding the dislocations (cf. Figs. 8 and 9) we note a stronger curvature of those rolls running through the pentagonal in comparison to those going through hexagonal cells. Thus there exists an asymmetry in the curvature, and consequently in the mean flow, with respect to the dislocation position. This fact might explain the existence of preferred direction of the glide/climb motion. The glide/climb process continues and we observe the appearance of a (2,4)-pentaline [Figs. 8(e)–8(h)].

With increasing order of the pentaline the distance of separation between both dislocations increases, too. While this distance was about two average hexagon side lengths for the 5-5-6-6 cluster it amounts to more than six side lengths for the (2,4)-pentaline. Note that the transformation of the 5-5-6-6 cluster into a (2,4)-pentaline proceeds parallel to the axis of mode 3 which remains free of dislocations during this process. The 5-5-6-6 cluster can be considered in this notation as a (0,2)-pentaline.

Before turning to the qualitative changes provoked by the growth of the pentalines we wish to consider a quantitative effect manifesting itself in an increase of orientational distorsion. To analyze this effect we use patterns with isolated defects only. By isolated we mean that the defect is embedded into a well ordered hexagonal pattern of about 140 hexagonal cells and separated from other defects by a distance comprising at least 10 hexagonal cells. We apply Fourier transformation to such sections of the pattern containing isolated defects to determine the angular position of the Fourier modes $\phi_i$ and finally the angle $\Delta\phi_{ij}=|\phi_i-\phi_j|$ between the modes $i$ and $j$ $(i\neq j)$. Clearly, in the purely hexagonal case all three angles are equal to $\Delta\phi_{ij}=120°$. The insert of a dislocation into a particular roll pattern should lead to a wider angular distribution of the Fourier components while the angular position of the center of mass of this mode remains unchanged. However, the behavior of the dislocations, as observed in the experiment, does not fit into this simple idea as shown in Fig. 10. Moreover, we find a monotonous increase of $\Delta\phi_{12}$ with increasing order of the pentalines at the expense of a shortening of $\Delta\phi_{13}$ and $\Delta\phi_{23}$. It is remark-

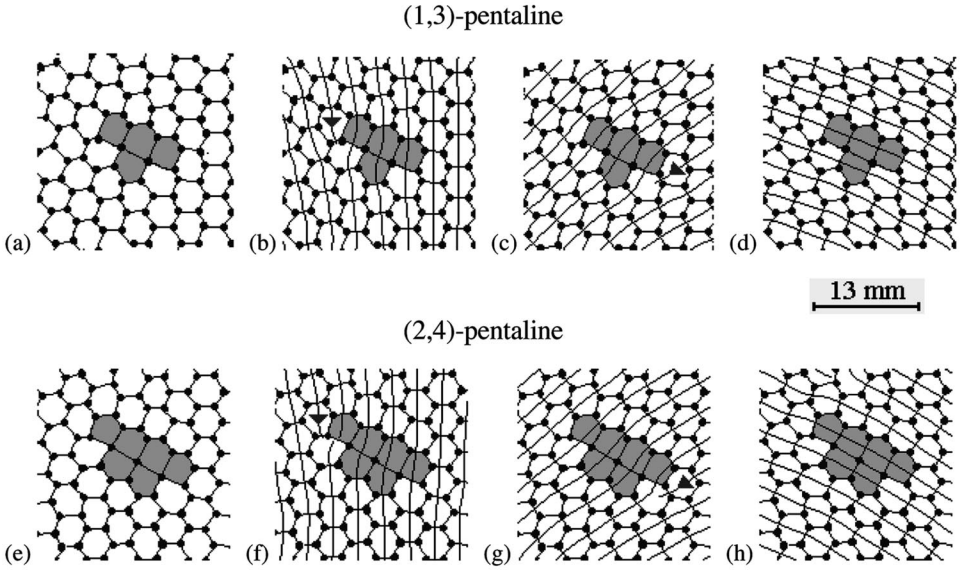


FIG. 8. The initial stage of pentalines: (1,3)-pentaline [(a)–(d)] and (2,4)-pentaline [(e)–(h)]. The transition from the 5-5-6-6 cluster into a (1,3)-pentaline and its transition into a (2,4)-pentaline proceeds similar to the closing of a zipfastener: The shortest side of one of the two outer non-equilateral hexagons vanishes. So, two new pentagons appear. This step is equivalent to the glide motion of one of the two dislocations by one $2\pi/k_i$ together with a climb motion by about one hexagon side length. For clear illustration the original shadowgraphs are again converted into binary pictures (cf. Fig. 5). The particular pentalines are shown in gray. Dislocated rolls are marked by arrows.

able that the angle $\Delta\phi_{12}$ is exactly that between the both modes containing the two dislocations. Thus, the glide motion changes significantly the orientation of the particular modes. This observation supports the idea that the gliding leads to a selection of the orientation [16,14,19]. However, with increasing order of the pentalines, i.e., beyond the (2,4)-pentaline, we observe a decrease of $\Delta\phi_{12}$ again and a corresponding increase of the other two angles. This is mostly due to escaping of one dislocation via the rim achieved by the radial alignment of the pentalines. But, unfortunately no systematic study of this effect was possible since the frequency to find sufficiently isolated pentalines of higher order is low, even at an aspect ratio of $\Gamma = 80$.

Here, a comment is in order with respect to the stability, i.e., the lifetime of these defects *in otherwise well ordered hexagonal patterns*. The stability of (0,2)-pentalines is comparable to that of a PHD. We have observed stationary (0,2)-pentalines for more than 60 hours. Pentalines of higher order than (1,3) have to be considered as metastable states. They can occur but they frequently decay into (0,2)-pentalines. However, the stability ratio between (0,2)-pentalines and higher-order pentalines reverses with increasing $\varepsilon$ whereby the latter become the dominant defect type. The stability of (1,3)-pentalines in a hexagonal matrix can presently not be definitely answered. We have traced (1,3)-pentalines over a duration of 8 hours.

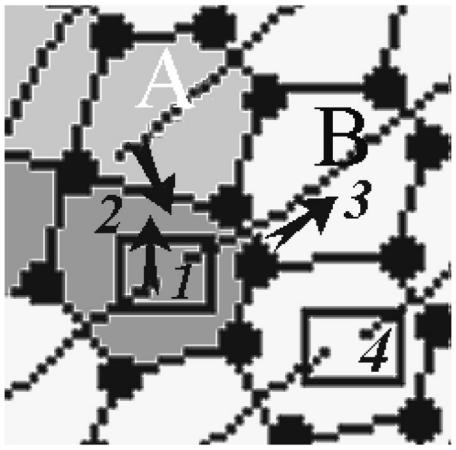


FIG. 9. The mechanism of the pentagon formation consists in a combination of glide (steps 1 and 2) and climb (step 3) motions. 1—pinching off of a roll somewhere within the shown rectangle, 2—reforming of a new roll by the movement of the originally dislocated roll (denoted by $A$) and the lower part of the pinched off roll towards each other. The direction of the movement is indicated by black arrows. 3—climb motion of the newly formed dislocation (denoted by $B$) causing the corresponding hexagon side to vanish. The next cycle of glide/climb motion is initiated by another pinching off denoted by 4. The figure shows an enlarged detail of Fig. 5(c).

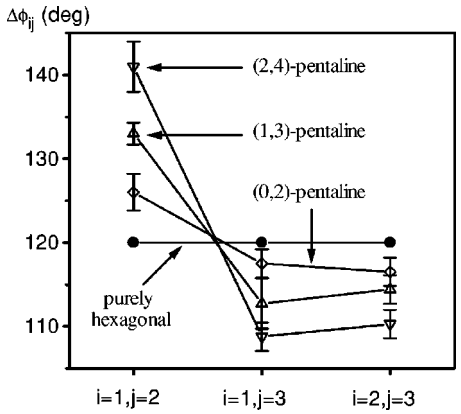


FIG. 10. The angle $\Delta\phi_{ij}$ between the three modes (numbered by $i$ and $j$) in presence of pentalines of various order. $\Delta\phi_{12}$ stands for the angle between the both roll sets containing the dislocations. Note the increase of this angle with increasing amount of pentagonal cells.

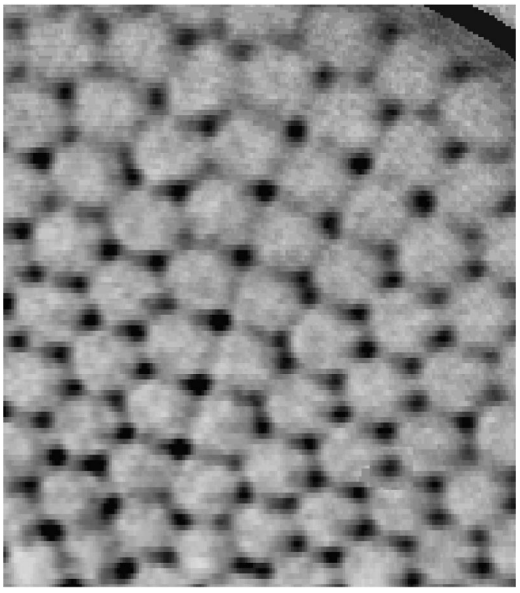

FIG. 11. The pentaline in a developed stage at $\varepsilon = 4.2$. In the upper part, close to the rim of the experimental container, an undoing of the pentaline occurs allowing the formation of square cells. This underlines the mediating character of the pentalines within the hexagon-square transition in surface-tension-driven Bénard convection.

We remark that, with view to the entire structure, a strict hierarchy in the sequence of the defects with increasing control parameter does not exist. That means, at a given $\varepsilon_1 > 2$ one will not see all PHD's converted into clusters, and for $\varepsilon_2 > \varepsilon_1$ all clusters into (1,3)-pentalines, etc. Moreover, we observe a coexistence of the various defects in different places of the experimental container over a wide range of $\varepsilon$ values. But, if a pentaline of a given order appears it exactly has evolved according to the schema sketched above.

We see two reasons for the coexistence of various defects. First, defects appear spontaneously in the course of pattern evolution. Therefore, the extent of defected regions varies across the experimental container. Consequently, the mean flow caused by the curvature of the rolls has locally a different strength. Since the mean flow is assumed as an important mechanism for the dislocation gliding the existence of defects of different order is plausible. Second, experimental inhomogeneities, such as an imperfect pinning of the meniscus, cannot completely be excluded. These perturbations give rise to weak temperature perturbations which, close to the rim, can produce a dynamics similar to that of the mean flow.

## V. FINAL STATE OF THE PENTALINE

The further development of the pentaline proceeds according to the sketched schema. However, we never observed in our experiments that a pentaline penetrates through the entire experimental container. The maximal length is of the order of the container radius $r$. At this stage, such a pentaline is comprised of about 10–16 pentagons, depending on the aspect ratio $\Gamma$. Natural boundaries against a nonlimited growth are grain boundaries and pentalines which grow from other regions with different orientation. As a rule, the pentalines are directed towards the rim in radial direction. This gives one dislocation the possibility to escape from the pattern via the rim. An example of a developed pentaline is given in Fig. 11.

The important aspect coming out of Fig. 11 is the formation of square cells between the both cords of pentagons of the pentaline. Hence, the advanced pentalines mediate the transition to square convection cells [5,7,8]. The process, leading to the formation of square cells, is the same as for the transformation of hexagons into pentagons. One of the outer sides of the pentagons become shorter and shorter till again both cell knots merge. This tendency is clearly visible in pentagons located at the right side in Fig. 11. The loss of stability of hexagonal cells, caused by the formation of the pentalines, can qualitatively be described in terms of a loss of phase synchronization. The hexagonal pattern is the product of the resonant three-wave-interaction which requires that $\phi_1 + \phi_2 + \phi_3 = 0$. $\phi_i$ stand for the phase of modes $i$. The region where this condition is not longer fulfilled increases with growth of the pentaline, i.e., with increasing distance of separation of the two dislocations. Cells of another planform, namely with square one, can appear in this region.

## VI. SUMMARY

With the pentalines a new class of defects appears in the higher supercritical hexagonal pattern. The nucleus of each of these defects is the decay of the basic penta-hepta defect. Similarly to the PHD, the pentaline involves two dislocation of opposite phase circulation. But, in contrast to the PHD, the dislocations are not longer bound together. Moreover, the distance of separation between both dislocation cores increases with increasing order of the pentaline. The basic mechanism, underlying the formation and evolution of the pentalines, is a combination of glide and climb motions of one or both dislocations. The pentalines are regions where the phase synchronization, required for the hexagonal pattern, is disturbed. This explains the mediating role which the pentalines play during the transition from hexagonal to square cells. The present study of the defects as function of the control parameters differs from the program conveniently applied, namely the measurement of the defect velocity as function of the wavenumber mismatch at constant $\varepsilon$. However, our study supports an intuitive understanding what the consequences of dislocation motion in hexagonal patterns are.

We hope that the description of the pentalines will stimulate both the theoretical modeling and new experimental work. Particularly useful seems to be a study of the influence of the Prandtl number on the glide velocity to understand the question of whether the amount of vertical vorticity created by the roll curvature, increases the glide velocity.

## ACKNOWLEDGMENTS

We are grateful to A. A. Nepomnyashchy, U. Thiele, M. Bestehorn, K. Neuffer, and M. Schatz for stimulating discussions. K. E. and A. T. acknowledge financial support from the Deutsche Forschungsgemeinschaft (Grant No. Th497/8-1) and from the Sächsisches Staatsministerium für Wissenschaft und Kunst.

[1] J.A. Whitehead, J. Fluid Mech. **75**, 715 (1976).
[2] A. Pocheau and V. Croquette, J. Phys. (France) **45**, 35 (1984).
[3] P. Coullet, L. Gil, and J. Lega, Physica D **37**, 91 (1989).
[4] I. Rehberg, S. Rasenat and V. Steinberg, Phys. Rev. Lett. **62**, 756 (1989).
[5] K. Nitschke and A. Thess, Phys. Rev. E **52**, 5772 (1995).
[6] M. Bestehorn, Phys. Rev. Lett. **76**, 46 (1996).
[7] K. Eckert, M. Bestehorn, and A. Thess, J. Fluid Mech. **356**, 155 (1998).
[8] U. Thiele and K. Eckert, Phys. Rev. E **58**, 3458 (1998).
[9] M. Schatz *et al*. (unpublished).
[10] M.C. Cross and P.C. Hohenberg, Rev. Mod. Phys. **65**, 851 (1993).
[11] E.D. Siggia and A. Zippelius, Phys. Rev. A **24**, 1036 (1981).
[12] G. Tesauro and M.C. Cross, Phys. Rev. A **34**, 1363 (1986).
[13] V. Croquette, M. Mory, and F. Schosseler, J. Phys. (France) **44**, 293 (1983).
[14] J. Millán-Rodriguez, M. Bestehorn, C. Peréz-García, R. Friedrich, and M. Neufeld, Phys. Rev. Lett. **74**, 530 (1995).
[15] L. Kramer and W. Pesch, Annu. Rev. Fluid Mech. **27**, 515 (1995).
[16] E. Bodenschatz, W. Pesch, and L. Kramer, Physica D **32**, 135 (1988).
[17] L. Kramer, E. Bodenschatz, W. Pesch, W. Thom, and W. Zimmermann, Liq. Cryst. **5**, 699 (1989).
[18] G. Goren, I. Procaccia, S. Rasenat, and V. Steinberg, Phys. Rev. Lett. **63**, 1237 (1989).
[19] S. Nasuno, S. Takeuchi, and Y. Sawada, Phys. Rev. A **40**, 3457 (1989).
[20] S. Rasenat, V. Steinberg, and I. Rehberg, Phys. Rev. A **42**, 5998 (1990).
[21] E. Braun and V. Steinberg, Europhys. Lett. **15**, 167 (1991).
[22] J. Pantaloni and P. Cerisier, in *Cellular Structures in Instabilities*, edited by J. E. Wesfreid and S. Zaleski (Springer Verlag, Berlin, 1984).
[23] P. Cerisier, C. Pérez-García, and R. Occelli, Phys. Rev. E **47**, 3316 (1993).
[24] P. Cerisier, S. Rahal, and N. Rivier, Phys. Rev. E **54**, 5086 (1996).
[25] S. Ciliberto, P. Coullet, J. Lega, E. Pampaloni, and C. Pérez-García, Phys. Rev. Lett. **65**, 2370 (1990).
[26] L.M. Pismen and A.A. Nepomnyashchy, Europhys. Lett. **24(6)**, 461 (1993).
[27] M.I. Rabinovich and L.S. Tsimring, Phys. Rev. E **49**, R35 (1994).
[28] L.S. Tsimring, Phys. Rev. Lett. **74**, 4201 (1995)
[29] L.S. Tsimring, Physica D **89**, 368 (1996).
[30] B. Jähne, *Digitale Bildverarbeitung* (Springer Verlag, Berlin, 1991).
[31] D. Bensimon, B.I. Shraiman, and V. Croquette, Phys. Rev. A **38**, 5461 (1988).
[32] H. Bénard, Rev. Gen. Sci. Pures Appl. **11**, 1261 (1900).